ISSN 1028-334X, Doklady Earth Sciences, 2007, Vol. 412, No. 1, pp. 43–48. © Pleiades Publishing, Ltd., 2007.
Original Russian Text © M.A. Mishkin, G.M. Vovna, A.M. Lennikov, V.G. Sakhno, Z.G. Badredinov, R.A. Oktyabr'skii, A.N. Solyanik, 2007, published in Doklady Akademii Nauk, 2007, Vol. 412, No. 3, pp. 373–378.

GEOLOGY

The Lower Crustal Early Proterozoic Metabasite–Enderbite Association of the Dzhugdzhur Block (Aldan Shield): Its Nature and Origin of Protoliths

M. A. Mishkin, G. M. Vovna, A. M. Lennikov, Corresponding Member of the RAS V. G. Sakhno, Z. G. Badredinov, R. A. Oktyabr'skii, and A. N. Solyanik

Received July 28, 2006

DOI: 10.1134/S1028334X07010102

The origin and growth of the continental crust is one of the main problems in the study of the Earth's history. At present, the composition of the continental crust is sufficiently well known for the Archean shields, where the crust is exposed. Study of the Early Proterozoic sialic crust encounters serious difficulties because its fields are usually less eroded as compared with Archean shields and are overlain by Upper Proterozoic–Phanerozoic formations. Researchers of Lower Proterozoic rocks on Archean cratons usually deal with either Early Proterozoic volcanosedimentary formations of greenstone belts related to intracratonic rifting or sedimentary fold–thrust complexes. The Early Proterozoic crust developed between Archean cratons is observable only in some tectonic windows. Of greatest interest among them are deep-rooted blocks of metamorphic rocks with exposed lower layers of the Early Proterozoic crust, the igneous protoliths of which provide information on the early stages of its formation. Deep metamorphism settings of rocks in these blocks are confirmed by geothermobarometric data.

We present the first data on the composition of the Early Proterozoic lower crust obtained for the Dzhugdzhur deep-seated block that was formerly considered an element of the Aldan Shield. In available tectonic maps, the Dzhugdzhur block is located in the southeastern part of the Aldan Shield in the Kun-Man'e, Ayumkan, and Maya river basins (Fig. 1). Based on published data and original field observations, we subdivided the stratified granulite complex of the Dzhugdzhur block into two sequences. The lower sequence is composed of hypersthene plagiogneiss–enderbites intercalated with two-pyroxene crystalline schists. The upper sequence consists largely of biotite–garnet, biotite, and biotite–graphite gneisses with interbeds of marbles and subordinate enderbites and two-pyroxene schists. Figure 1 demonstrates the distribution of these sequences. We define the lower sequence as the metabasite–enderbite association. This paper is dedicated to description of this association.

According to geothermobarometric data, rocks of the Dzhugdzhur block were metamorphosed under conditions of granulite facies at $T = 800°C$ and $P = 9$ kbar [1]. The Dzhugdzhur Complex was previously assigned to the Archean, although isotopic dating was not carried out. We obtained the first data on Sm–Nd systematics of metabasite–enderbite rocks of the complex, which indicate its Early Proterozoic age.

Using the technique described in [2], we revealed petrochemical properties and regularities in the distribution of trace elements in granulites of the Dzhugdzhur Complex and, thus, the geological nature of their protoliths. The data obtained imply that the lower and upper sequences were composed primarily of volcanogenic and volcanosedimentary rocks, respectively. Primary volcanics of the lower sequence are attributed to three petrochemical series: calc-alkaline, komatiite–tholeiitic, and picritic. The primary volcanic association of the calc-alkaline petrochemical series includes basalts, basaltic andesites (two-pyroxene crystalline schists), and andesites (enderbites). Basaltic andesites and andesites are dominant. The komatiite–tholeiitic series is represented by the association of tholeiitic and komatiite–tholeiitic basalts and komatiites (two-pyroxene, two-pyroxene–amphibole, and olivine–two-pyroxene crystalline schists). Tholeiitic basalts are dominant among volcanics of the primary association. The picritic association consists only of picritic basalts (two-pyroxene crystalline schists) that have limited distribution.

Far East Geological Institute, Far East Division, Russian Academy of Sciences, pr. Stoletiya Vladivostoka 159, Vladivostok, 690022 Russia;
e-mail: galochka@mail.primorye.ru

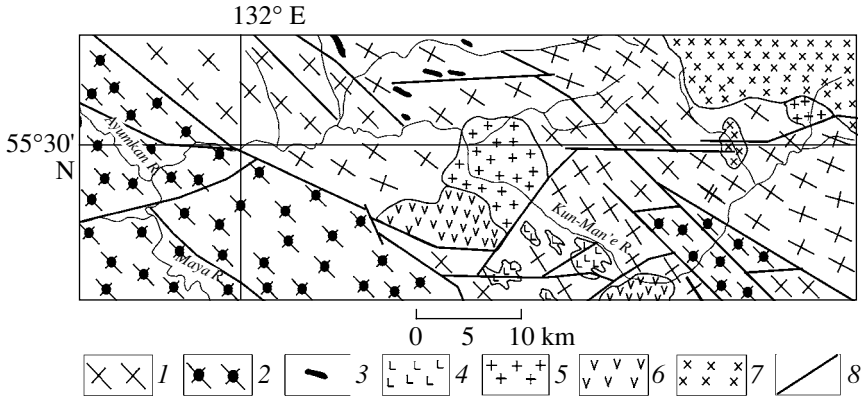

Fig. 1. Schematic geological map of the study area (based on published data and original field observations by A.M. Lennikov, M.A. Mishkin, and R.A. Oktyabr'skii). (*1, 2*) Dzhugdzhur granulite complex: (*1*) granulites of the lower sequence (enderbites, metabasites), (*2*) granulites of the upper sequence (alumina gneisses, enderbites, metabasites, calciphyres); (*3–5*) Lower Proterozoic metamorphic intrusive rocks: (*3*) metamorphic ultramafics and basites, (*4*) anorthosites, (*5*) granites; (*6*) platform cover; (*7*) Cretaceous granitoids; (*8*) tectonic dislocations.

The Al–(Fe + Ti)–Mg classification diagram (Fig. 2) demonstrates the chemical compositions of the main varieties of granulite rocks belonging to the metabasite–enderbite association. Table 1 presents their average values.

Basaltic andesites and andesites of the calc-alkaline series are present in approximately equal proportions. They are sharply dominant among primary volcanics of the lower sequence. The igneous protolith of the upper volcanosedimentary sequence includes basalts, basaltic andesites (two-pyroxene crystalline schists), and andesites (enderbites) of the calc-alkaline series.

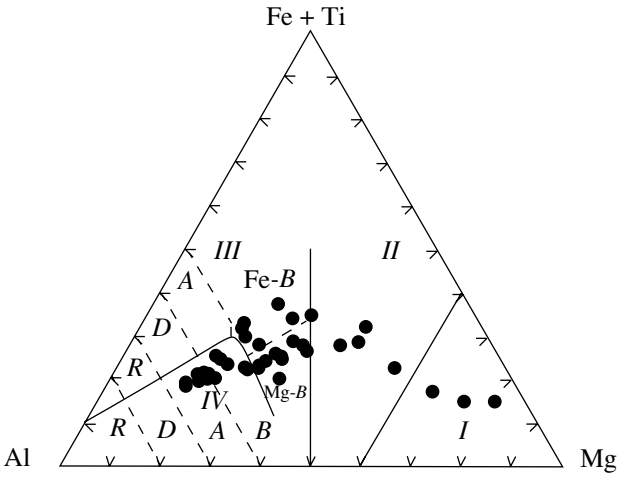

Fig. 2. Al–(Fe + Ti)–Mg classification diagram (at %). Dots show compositions of granulites from the metabasite–enderbite association of the Dzhugdzhur Complex. Rock fields: (*I*) komatiites, (*II*) komatiitic and high-magnesian basalts, (*III, IV*) volcanics of tholeiitic (*III*) and calc-alkaline (*IV*) series. Rock types: (*R*) rhyolites; (*D*) dacites; (*A*) andesites; (*B*) basalts: (Fe-*B*) high-ferrous, (Mg-*B*) high-magnesian.

In the multielement diagram (Fig. 3), metaandesites (enderbites) of the calc-alkaline series from the Dzhugdzhur Complex are generally similar (in terms of the content of rare elements) to "gray gneisses" constituting the basement of Archean shields [3]. However, the Th and Zr concentrations are lower.

Two-pyroxene schists and enderbites from the metabasite–enderbite association, which correspond in their primary composition to basaltic andesites and andesites, respectively, were studied by the Sm–Nd isotopic method (Table 2). The T_{DM} values obtained for the analyzed rocks suggest the formation of their protoliths in the Early Proterozoic. Positive $\varepsilon_{Nd}(T)$ values indicate the juvenile origin of primary volcanics from the basalt–andesite association of the Dzhugdzhur Complex.

Many researchers attribute the origin of primary melts of the "gray gneissic" sialic crust to partial melting of the mafic source, which is confirmed by numerous experimental data. At present, the majority of geologists believe that the sialic crust of the tonalite–trondhjemite–granodiorite composition (TTG "gray gneisses") is a product of melting of the primary basaltic crust by the heat of ascending mantle plumes. In [2], we studied the deep-seated metabasite–enderbite complex of the Sutam block (Aldan Shield) and demonstrated that the plume model of the early sialic crust formation may also be valid for the Late Archean.

Based on available published isotopic dates, we can identify three Archean (Siberian, China, and Omolon–Okhotsk) cratons in eastern Asia (Fig. 4). The Omolon–Okhotsk Craton comprises the Okhotsk and Omolon massifs, which represent, in our opinion, a single structure.

In the Early Proterozoic (2.5–1.65 Ga), the sialic crust continued to form around Archean cratons of the future Asian continent owing to the amalgamation of the primary basaltic crust.

Table 1. Average chemical compositions of metavolcanic rocks from the metabasite–enderbite association of the Dzhugdzhur granulite complex

Component	1	2	3	4	5	6	7
	Metakomatiite	Komatiitic metabasalt	Tholeiitic metabasalt	Picritic metabasalt	Metabasalt	Basaltic metaandesite	Metaandesite
SiO_2	47.06	44.64	50.10	48.39	49.30	54.80	58.4
TiO_2	0.52	0.86	1.16	1.62	0.77	0.67	0.67
Al_2O_3	3.61	12.67	14.11	11.92	18.26	17.93	16.07
Fe_2O_3	2.83	4.64	3.3	3.97	3.59	3.90	2.79
FeO	8.66	9.68	9.20	10.21	6.72	4.71	5.21
MnO	0.22	0.17	0.30	0.19	0.12	0.14	0.14
MgO	24.68	11.61	7.08	9.14	6.72	4.18	3.72
ëaO	6.73	10.29	10.02	10.21	9.42	7.46	6.42
Na_2O	0.93	1.65	2.83	2.43	2.91	4.12	3.73
K_2O	0.42	1.01	0.64	0.90	0.89	1.26	1.44
P_2O_5	0.06	0.68	0.35	0.59	0.29	0.36	0.31
L.O.I.	1.19	2.10	0.92	0.69	1	0.47	0.62
U	0.22	0.07	0.11	0.10	0.16	0.03	0.20
Th	0.38	0.28	0.49	0.61	0.57	0.15	0.90
Ba	10.00	236.87	206.87	522.33	315.72	604.90	502.88
Sr	38.375	546.93	345.41	450.75	563.56	806.63	644.55
La	2.33	15.72	19.25	34.86	15.13	22.59	20.72
Ce	6.34	38.36	46.93	79.82	33.57	49.98	44.91
Pr	0.96	5.66	6.57	10.98	4.55	6.67	5.95
Nd	4.62	24.82	26.99	46.48	18.34	27.82	24.21
Sm	1.38	5.41	5.70	9.63	3.77	5.47	4.71
Eu	0.54	1.60	1.66	2.31	1.22	1.88	1.20
Gd	1.77	5.30	5.38	9.40	3.7	4.82	4.33
Tb	0.29	0.78	0.86	1.45	0.58	0.77	0.71
Dy	1.71	3.96	4.45	6.84	2.98	3.66	3.49
Ho	0.36	0.80	0.91	1.36	0.60	0.74	0.71
Er	1.04	2.32	2.77	4.01	1.76	2.17	2.06
Tm	0.14	0.30	0.38	0.52	0.23	0.30	0.29
Yb	0.92	1.93	2.47	3.25	1.52	1.91	1.89
Lu	0.14	0.28	0.37	0.46	0.22	0.29	0.29
Zr	23.77	41.36	47.58	63.13	38.73	28.88	30.94
Hf	0.73	1.27	1.42	2.22	1.13	0.99	0.74
Ta	0.10	0.34	0.43	0.65	0.46	0.41	0.53
Nb	0.82	4.23	6.95	13.93	4.57	6.21	8.64
Y	8.485	19.60	22.92	34.97	14.62	17.74	16.82
Sc	31.10	40.20	38.92	41.41	24.27	21.78	19.25
Ni	745.385	141.19	112.74	87.91	41.71	32.94	35.51
Co	94.59	64.65	47.94	55.62	42.31	26.20	21.88
V	145.90	265.97	220.42	286.01	216.27	155.80	141.15

Note: Oxides are given in wt %; trace elements, in ppm. All analyses are adjusted to the sum of main petrogenic oxides equal to 100%. (1–3) Metavolcanics of the komatiite–tholeiitic series; (4) metabasalts of the picritic series; (5–7) metavolcanics of the calc-alkaline series.

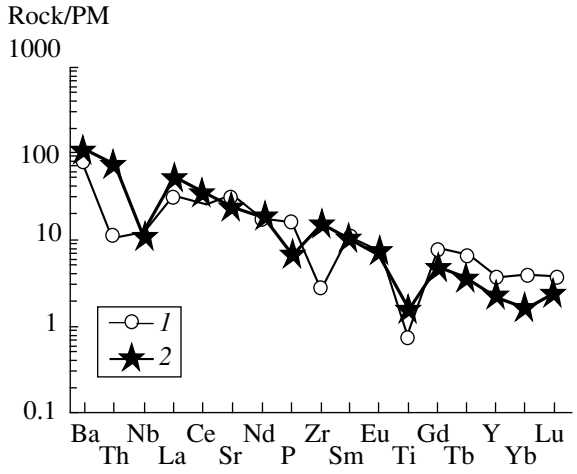

Fig. 3. Multielement diagram for metaandesites from the metabasite–enderbite association of the Dzhugdzhur Complex. (*1*) Metaandesites of the Dzhugdzhur Complex; (*2*) Archean "gray gneisses" [3]. Normalized to the primitive mantle (PM) composition.

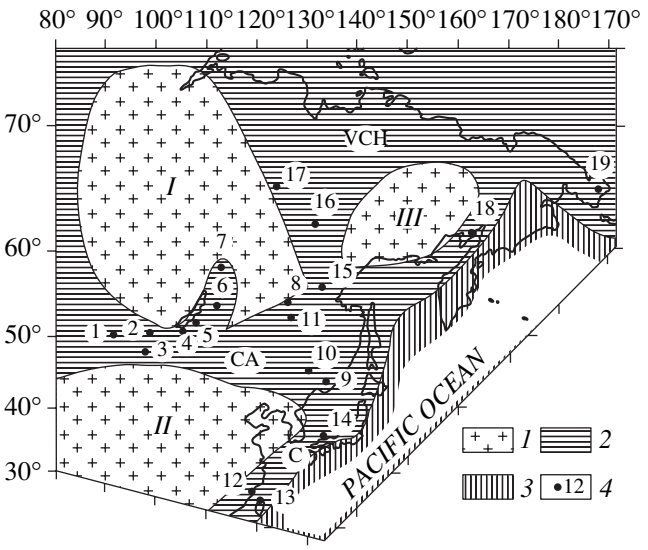

Fig. 4. Schematic distribution of the Early Proterozoic crust in eastern Asia. (*1*) Archean sialic crust; (*2*) Early Proterozoic sialic crust; (*3*) assumed distribution of the Riphean and Early Proterozoic newly formed sialic crust; (*4*) sampling points of Lower Proterozoic rocks for isotopic dating. (*I–III*) Archean cratons: (*I*) Siberian, (*II*) China, (*III*) Omolon–Okhotsk. Fold belts: (CA) Central Asian, (VCH) Verkhoyansk–Chukotka, (C) Catasian.

As was shown in [2], study of the lower sialic crust in natural sections is important for substantiating the formation model of "gray gneissic" primary melts. On all continents, these sections are characterized by intercalation of primary volcanics of the komatiite–tholeiitic and calc-alkaline series in granulite complexes. The upper parts of the sections lack komatiites and usually consist of volcanics of the calc-alkaline series (andesite–dacite association) [2]. Such a relationship of primary volcanics in the lower crustal sialic sections may be explained only in terms of the mantle plume model. According to [2], formation of the matabasite–enderbite association protolith includes two stages. The first stage is marked by the formation of volcanics of the komatiite–basaltic association owing to the partial decompression melting of material of the ascending mantle plume. During the second stage, volcanics of the andesite–dacite association are formed as the result of partial melting of the primary basaltic crust by the heat of the ascending mantle plume and its magmatic offshoots. The principle similarity between the primary section of the Dzhugdzhur Complex and the section of the Upper Archean Sutam Complex described in [2] allows us to accept the plume model for the formation of the volcanics of the Dzhugdzhur Complex. The depleted upper mantle served as a source for the plume.

The isotope data available now for metamorphic and igneous complexes of eastern Asia make it possible to outline the inferred domain of the Early Proterozoic continental crust (Fig. 4).

In the western part of the Central Asian foldbelt, Lower Precambrian rocks are defined in the Dzabkhan microcontinent, Gargan block, and Tuva–Mongol Massif. The Archean age of metamorphic rocks from the Baidarik block of the Dzabkhan microcontinent and

Table 2. Results of the Sm–Nd study of two-pyroxene schists and enderbites of the Dzhugdhur Complex

Sample	Nd (ppm)	Sm (ppm)	$^{143}Nd/^{144}Nd$	$^{147}Sm/^{144}Nd$	T_{DM}	$\varepsilon_{Nd}(T)$
E-17/158	26.38	5.45	0.511772	0.1248	2356	5.30
E-17/159	43.13	7.77	0.511566	0.1089	2298	6.18
E-35/296	16.96	3.28	0.511435	0.1169	2689	1.15
E-41/339	16.70	1.93	0.511452	0.0997	2264	6.80

Note: Sm and Nd isotopic measurements were carried out by G.M. Vovna under the supervision of Prof. D. Maeda at the University of Hokkaido using a Finnigan MAT-262 multichannel mass spectrometer. $\varepsilon_{Nd}(T)$ values are calculated for $T = 2400$ Ma. (E-171/158, E-17/159, E-35/296) two-pyroxene schists; (E-41/339) enderbite.

Gargan block is substantiated by isotopic dates [4]. We include them into the China and Siberian cratons, respectively, in Fig. 4. The Early Precambrian basement of the Tuva–Mongol Massif is overlain by the Riphean–Vendian sedimentary complex. According to [4], Upper Riphean–Vendian metamorphic rocks of the sedimentary complex overlying the Tuva–Mongol Massif contain rare grains of detrital zircons with Early Proterozoic nuclei (1935 ± 21 and 2557 ± 34 Ma, SHRIMP-II; Fig. 4, point 1). The Sm–Nd studies confirm these results. Some rock varieties from this fold–thrust complex are characterized by the Early Proterozoic Nd model age of 1.8–2.2 Ga and negative $\varepsilon_{Nd}(T)$ values. This implies an admixture of Lower Proterozoic crustal material derived from the basement of the Tuva–Mongol Massif in primary Upper Riphean–Vendian sedimentary rocks.

In [5], data on Sm–Nd systematics in the Phanerozoic granitoids from fold structures around the southern Siberian Craton and western Transbaikal region are summarized. The materials indicate the existence of the Early Proterozoic stage in the crust formation (Fig. 4, points 2–6). The presence of outcrops of Lower Proterozoic rocks in the Patom–Bodaibo structural zone supports this inference (Fig. 4, point 7).

In the eastern part of the Central Asian foldbelt, Lower Proterozoic rocks are known in the Bureya Massif (Gonzha block, 2160 ± 100 Ma, U–Pb method; Fig. 4, point 8) [6], Khankai Massif (Sergeevo block, 2471 ± 0.08 and 2106 ± 0.07 Ma, Rb–Sr method; Fig. 4, point 9) [7], and Jiamusy Massif (China) (Mashan block, 2275 Ma, U–Pb method; Fig. 4, point 11) [8]. It should be noted that metamorphic rocks of the Late Riphean–Vendian fold–thrust complex in the Jiamusy Massif contain single grains of detrital zircons, with nuclei dating back to 1675–1900 Ma (SHRIMP method) [9]. The presence of the Early Proterozoic sialic crust at the base of the eastern Central Asian belt is also evident from finds of xenogenic Early Proterozoic zircon grains within Phanerozoic granitoids. This can be exemplified by finds of xenogenic zircons (2215 ± 7 Ma, SHRIMP-II method) [10] in Jurassic granites of the Bureya Massif (Mamyn block, Fig. 4, point 11).

The Catasian foldbelt represents a southern branch of the Central Asian belt in eastern Asia. In this area, blocks of Lower Proterozoic rocks are known from the southeastern coast of China (1689 and 1761 Ma, U–Pb method) [11], the Island of Taiwan (2087 Ma, U–Pb method, Fig. 4, points 12, 13) [11], and the Hida zone of Japan (1960 Ma, U–Pb method, Fig. 4, point 14) [12].

We attribute granulites of the Dzhugdzhur block in the Verkhoyansk–Chukotka fold zone to the Early Proterozoic basement of the fold zone (Fig. 4, point 15). North of the Dzhugdzhur block, Lower Proterozoic rocks were recovered by boreholes beneath the sedimentary Verkhoyansk Complex (Fig. 4, points 16, 17) [13]. In the folded structures surrounding the eastern Omolon–Okhotsk Craton, metamorphic rocks developed in the Avekova River basin of the Taigonos Peninsula are referred to the Early Proterozoic (1737 ± 68 Ma, U–Pb method, Fig. 4, point 18) [14]. Spacious outcrops of Lower Proterozoic crystalline rocks (1990 ± 150 Ma, Rb–Sr method, Fig. 4, point 19) [15], which correlate with isotopically dated Lower Proterozoic formations of Alaska, are known in the Chukotka Massif.

Processes of Early Proterozoic crust formation resulted in amalgamation of Archean cratons into a single protocontinent that represented a major element of Pangea.

Two main geotectonic regimes were in action during the Riphean and Phanerozoic in areas of Early Proterozoic crust development: intracontinental rifting and the regime of epicontinental seas. In terms of the extension degree of the crust, rifts did not exceed the opening stage of the present-day Red Sea. Riftogenic magmatism in them was induced by plume formation in the depleted upper mantle. The products of this process are represented by ultramafic and mafic rocks of the tholeiitic series (ophiolites, according to some authors), coupled with basic, intermediate, and acid rocks of the calc-alkaline series (“island-arc” series, according to some authors). Alkalic magmatism of that time indicates displacement of some magmatic plume sources to the undepleted lower mantle.

The Riphean–Paleozoic terrigenous and terrigenous–carbonate fold–thrust complex was formed by sediments of epicontinental seas.

Available geological and isotopic–geochemical data imply that the early sialic crust continued to form from basaltic rocks in the western Pacific at that time (Fig. 4). Discussion of these processes is, however, beyond the scope of this communication.

REFERENCES

1. O. V. Avchenko, *Mineral Equilibriums in Metamorphic Rocks and Problems of Geothermobarometry* (Nauka, Moscow, 1990) [in Russian].
2. M. A. Mishkin, G. M. Vovna, S. N. Lavrik, and R. A. Oktyabr’skii, Geochem. Int. **39**, 627 (2001) [Geokhimiya **39**, 691 (2001)].
3. H. Martin, *Archean Crustal Evolution,* Ed. by K.C. Condie (Elsevier, Amsterdam, 1994).
4. I. K. Kazakov, E. B. Sal’nikova, A. Natman, et al., Stratigr. Geol. Correlation **13**, 1 (2005) [Stratigr. Geol. Korrelyatsiya **13**, 3 (2005)].
5. V. V. Yarmolyuk, V. I. Kovalenko, V. P. Kovach, et al., Geotectonics **33**, 271 (1999) [Geotektonika **33** (4), 3 (1999)].
6. *Geological Map of the Amur River Region and Adjacent Areas, 1 : 2500000. Explanatory Notes*, Ed. by L.I. Krasnyi and Peng Yung Byao (St. Petersburg, 1999) [in Russian].
7. S. V. Kovalennko and I. A. Davydov, Dokl. Akad. Nauk **319**, 1173 (1991).

8. *Tectonic Framework and Crust Evolution of Eastern Jilin and Heilongjiang Provinces*, Ed. by C. Yijing and D. Zengxin (Laoning Univ. Press, Shenyang, 1996).
9. S. A. Wille, X. Zhang, and F. Wu, Tectonophysics **328** (1/2), 115 (2000).
10. A. A. Sorokin, N. M. Kudryashov, Li Tsingi, Tikhookean. Geol. **23** (5), 54 (2004).
11. T. F. Yui, L. Heaman, and C. Y. Lan, Tectonophysics **263** (1/4), 61 (1996).
12. K. Yamashita and T. Yanagi, Geochem. J. **28**, 333 (1994).
13. V. P. Kovach, A. B. Kotov, A. P. Smelov, et al., Petrology **8**, 353 (2000) [Petrologiya **8**, 399 (2000)].
14. E. A. Landa, B. A. Marovskii, S. S. Shevchenko, et al., in *Materials of the All-Russia Meeting "Geodynamics, Magmatism, and Mineralogy of North Pacific Continental Margins"* (SVKNII DVO RAN, Magadan, 2003), Vol. 2, pp. 139–142 [in Russian].
15. I. L. Zhulanova, *Earth's Crust of Northeastern Asia in the Precambrian and Phanerozoic* (Nauka, Moscow, 1990) [in Russian].